

A Unified Framework for Rethinking Policy Divergence Measures in GRPO

Qingyuan Wu^{1,2*} Yuhui Wang^{3*} Simon Sinong Zhan⁴ Yanning Dai³ Shilong Deng⁵ Sarra Habchi²
 Qi Zhu⁴ Matthias Gallé² Chao Huang¹

Abstract

Reinforcement Learning with Verified Reward (RLVR) has emerged as a critical paradigm for advancing the reasoning capabilities of Large Language Models (LLMs). Most existing RLVR methods, such as GRPO and its variants, ensure stable updates by constraining policy divergence through clipping likelihood ratios. This paper introduces a unified clipping framework that characterizes existing methods via a general notion of policy divergence, encompassing both likelihood ratios and Kullback-Leibler (KL) divergences and extending to alternative measures. The framework provides a principled foundation for systematically analyzing how different policy divergence measures affect exploration and performance. We further identify the KL3 estimator, a variance-reduced Monte Carlo estimator of the KL divergence, as a key policy divergence constraint. We theoretically demonstrate that the KL3-based constraint is mathematically equivalent to an asymmetric ratio-based clipping that reallocates probability mass toward high-confidence actions, promoting stronger exploration while retaining the simplicity of GRPO-style methods. Empirical results on mathematical reasoning benchmarks demonstrate that incorporating the KL3 estimator into GRPO improves both training stability and final performance, highlighting the importance of principled policy divergence constraints in policy optimization.

1. Introduction

Reinforcement Learning (RL) (Kaelbling et al., 1996; Sutton & Barto, 2018) has served as a pivotal training paradigm in decision-making problems (Tesauro, 1994; Silver et al., 2016; Mnih et al., 2013; Berner et al., 2019), and has re-

cently been playing a central role in advancing Large Language Models (LLMs) (Ouyang et al., 2022; Lambert et al., 2024). RL provides an efficient and general training framework for LLMs, enabling optimization over complex, non-differentiable objectives that extend beyond direct supervised learning from human data. This capability is particularly critical for real-world tasks such as code generation (Jain et al., 2024), mathematical reasoning (Zhang et al., 2024; Cobbe et al., 2021), and dialogue alignment (Chiang et al., 2024).

Current RL methodologies for LLMs, particularly in RL with Verified Reward (RLVR) (Lambert et al., 2024) settings, predominantly rely on Proximal Policy Optimization (PPO) (Schulman et al., 2017). PPO ensures training stability through the ratio-based clipping mechanism, aiming to approximate the trust-region constraint of Trust Region Policy Optimization (TRPO) (Schulman et al., 2015a). Recently, Group Relative Policy Optimization (GRPO) (Shao et al., 2024) has emerged as a memory-efficient alternative for training large-scale LLMs by using group-normalized returns as the advantage baselines, thus eliminating the need to maintain a separate value function. Like PPO, GRPO and its variants (Yu et al., 2025; Yang et al., 2025b) rely on the ratio-based clipping to ensure stable policy updates.

Despite their success, the reliance on ratio-based clipping constitutes a specific and potentially restrictive design choice within the broader landscape of policy optimization. While these methods aim to ensure stable updates by constraining policy divergences through clipping likelihood ratios, recent studies (Cui et al., 2025; Park et al., 2025) reveal that both training exploration and evaluation performance are highly sensitive to the specific definition and implementation of policy divergence constraints. Although different variants of the ratio-based clipping mechanism (Yu et al., 2025; Yang et al., 2025b) have been proposed, a principled understanding of how different policy divergence measures and corresponding constraints affect the trade-off between exploration and stability remains largely unexplored.

To address this issue, this paper first introduces a unified clipping framework that characterizes existing clipping methods under a general notion of policy divergence. This unified clipping framework provides a foundational perspective

*Equal contribution ¹University of Southampton ²Cohere
³KAUST ⁴Northwestern University ⁵University of Liverpool. Correspondence to: Qingyuan Wu <qingyuan.wu@soton.ac.uk>.

for analyzing various policy divergence constraints, encompassing both likelihood ratios and Kullback–Leibler (KL) divergences. Furthermore, we identify that the KL3 estimator (Schulman, 2020) serves as the pivotal policy divergence constraint under our framework. We theoretically demonstrate that the KL3-based constraint is mathematically equivalent to an asymmetric ratio-based clipping. Based on these observations, we propose Approximate Trust Region-based GRPO (ATR-GRPO). Unlike standard symmetric ratio-based clipping, ATR-GRPO leverages the KL3 estimator to actively steer exploration by reallocating probability mass toward high-confidence actions, all while maintaining the computational efficiency of GRPO. Comprehensive experiments on mathematical reasoning benchmarks demonstrate that KL3 estimator consistently improves training stability and final performance compared to existing state-of-the-art (SOTA) baselines. Our contributions can be summarized as follows:

- We introduce a unified clipping framework for policy optimization that unifies existing policy divergence constraints and can be extended to arbitrary alternative measures.
- We identify the KL3 estimator as an effective policy divergence constraint, establish its connection to ratio-based constraints, and theoretically show that it promotes stronger exploration than existing alternatives.
- Building on these insights, we develop ATR-GRPO, which exhibits improved exploration dynamics while retaining the simplicity of existing methods.
- We empirically show that ATR-GRPO enhances learning stability and achieves performance competitive with various SOTA baselines.

2. Related Work

RL for LLMs. Reinforcement Learning (RL) has been established as the standard paradigm for advancing Large Language Models (LLMs), such as RLVR (Lambert et al., 2024). PPO (Schulman et al., 2017) utilizes a clipped surrogate objective to ensure stable policy updates. However, PPO requires training a separate critic model, which can be prohibitive for large-scale reasoning tasks. To mitigate these memory constraints, RLOO (Ahmadian et al., 2024) eliminates the critic by employing the Leave-One-Out baseline to reduce variance by averaging rewards across other samples within the batch. GRPO (Shao et al., 2024) calculates advantages relative to a sampled group of outputs for each prompt, effectively optimizing memory usage for reasoning tasks. GSPO (Zheng et al., 2025) further extends this paradigm by elevating the optimization granularity to the sequence level, aligning updates with reward signals.

Building on GRPO or GSPO, some recent works such as GTPO (Tan et al., 2025) and EMPO (Zhang et al., 2025a) incorporate semantic entropy into reward shaping to address the persistent challenge of sparse credit assignment.

Trust Region Methods in RL. Trust-region methods underpin stable policy optimization in RL, from NPG (Kakade, 2001) to the explicit KL-constrained formulation of TRPO (Schulman et al., 2015a). However, TRPO relies on computationally expensive second-order optimization, making it impractical for large-scale RL tasks. To address this scalability issue, PPO (Schulman et al., 2017) was introduced as a first-order approximation that replaces the hard KL constraint with a ratio-based clipping, aiming to implicitly constrain policy updates. While PPO has become the de facto choice for large-scale training due to its computational efficiency, its reliance on ratio-based clipping does not explicitly enforce a trust-region constraint. Prior work has shown that this approximation can fail to properly control policy updates, leading to potential optimization instability, as demonstrated by TRGPO and Truly PPO (Wang et al., 2019; 2020). In this work, we propose a unified clipping framework that generalizes different policy divergence constraints, including likelihood ratios and KL divergences.

Clipping Mechanisms in RL. TRGPO (Wang et al., 2019) shows that ratio-based clipping in PPO overly constrains low-likelihood probabilities, and introduces dynamic clipping to relax this effect. Truly PPO (Wang et al., 2020) further exposes the divergence between ratio-based and KL-based constraints, and proposes a KL-based clipping method as an alternative. DAPO (Yu et al., 2025) introduces an asymmetric clip-higher mechanism that increases the upper clipping range, mitigating entropy collapse and facilitating probability increases for low-likelihood exploratory tokens. DCPO (Yang et al., 2025b) proposes the dynamic ratio-based clipping mechanism, which can adaptively adjust the clipping ranges based on the prior probabilities to strengthen exploration ability. Aside from exploration purposes, the dual clipping mechanism (Ye et al., 2020) is proposed to ensure the convergence and stability in large-scale distributed RL training of MOBA games, which is also adopted as the default technique in the LLM training framework (Sheng et al., 2025). SAPO (Gao et al., 2025) presents the soft gate operation to replace the hard clipping, stabilizing the optimization. These ratio-based clipping mechanisms, however, designed for stability, exert a profound and often detrimental influence on policy entropy (Cui et al., 2025; Park et al., 2025). Different from previous approaches, this paper identifies the KL3 estimator (Schulman, 2020) as the pivotal policy divergence constraint within our proposed framework, demonstrated by our theoretical analysis and empirical evaluation.

Table 1. Comparative analysis of policy divergence constraints. Unlike previous methods that rely on either heuristic symmetric ratio-based clipping (PPO, GRPO), asymmetric ratio-based clipping (DAPO) or computationally expensive full expectation of the KL divergence (TRPO, Truly PPO), our ATR-GRPO achieves a principled, approximate trust-region constraint with low computational cost.

Method	Clipping / Constraint Criterion	Trust-Region Constraint?	Computational Cost
PPO (Schulman et al., 2017), GRPO (Shao et al., 2024)	$w_t(\theta) \in [1 - \epsilon, 1 + \epsilon]$	✗	Low
DAPO (Yu et al., 2025)	$w_t(\theta) \in [1 - \epsilon_l, 1 + \epsilon_u]$	✗	Low
DCPO (Yang et al., 2025b)	$w_t(\theta) \in [0.5 + \frac{1}{2}\sqrt{\max(1 - \frac{4\epsilon_l}{\pi_{\theta_{\text{old}}}}, 0.5 + \frac{1}{2}\sqrt{1 + \frac{4\epsilon_u}{\pi_{\theta_{\text{old}}}}})}]$	✗	Low
TRPO (Schulman et al., 2015a)	$\text{KL}_t(\theta) \leq \delta$	✓	High
TRGPPO (Wang et al., 2019)	$w_t(\theta) \in [\min(u_{\delta}^{\text{KL}}, 1 - \epsilon), \max(u_{\delta}^{\text{KL}}, 1 + \epsilon)]$	✓	Medium
Truly PPO (Wang et al., 2020)	$\text{KL}_t(\theta) \leq \delta$	✓	Medium (for large action space $ \mathcal{A} $)
ATR-GRPO (ours)	$\text{KL}_3(\theta) \leq \delta$ or $w_t(\theta) \in [l_{\delta}^{\text{KL}3}, u_{\delta}^{\text{KL}3}]$	✓ (approximated by KL_3)	Low

3. Preliminaries

Language Model Generation as MDP. Language generation process can be formulated as a Markov Decision Process (MDP), denoted by the tuple $(\mathcal{S}, \mathcal{A}, \mathcal{T}, r)$. Here, \mathcal{S} denotes the state space, where the state at timestep t is defined as $s_t \triangleq (x, y_{<t})$, corresponding to the concatenation of the input query x and the partially generated response $y_{<t}$. The action space \mathcal{A} is defined over the token vocabulary, \mathcal{T} represents the transition dynamics induced by autoregressive token generation, and the reward function r is defined over concatenations of the input query x and the partially generated response. The policy π_{θ} parameterized by θ aims to maximize the objective $J(\theta)$ defined as:

$$J(\theta) = \mathbb{E}_{x \sim \mathcal{D}} \left[\mathbb{E} \left[\sum_t r(s_t, y_t); \pi_{\theta} \right] - \beta \text{KL}(\pi_{\theta}(\cdot|s_t) || \pi_{\text{ref}}(\cdot|s_t)) \right], \quad (1)$$

where \mathcal{D} denotes the query distribution, and y is the response generated by the language model π_{θ} . π_{ref} is a reference policy, KL denotes the Kullback–Leibler (KL) divergence between two policies (e.g., π_1 and π_2), defined as follows:

$$\text{KL}(\pi_1(\cdot|s) || \pi_2(\cdot|s)) \triangleq \sum_{a \in \mathcal{A}} \pi_1(a|s) \log \frac{\pi_1(a|s)}{\pi_2(a|s)}, \quad (2)$$

and β controls the KL regularization to avoid policy drift (Shao et al., 2024).

Clipping in Policy Optimization Algorithms. Given a query x and a generated response y , the clipped surrogate objective for the policy π_{θ} is defined as:

$$\mathcal{L}(\theta) = \mathbb{E}_{\substack{y \sim \pi_{\theta}(\cdot|x) \\ x \sim \mathcal{D}}} [\min(w_t(\theta)A_t, \text{clip}(w_t(\theta), \cdot)A_t)],$$

where $w_t(\theta) = \frac{\pi_{\theta}(y_t|s_t)}{\pi_{\theta_{\text{old}}}(y_t|s_t)}$ represents the token-level likelihood ratio between π_{θ} and old policy $\pi_{\theta_{\text{old}}}$. Here, the term A_t denotes the advantage estimate, which corresponds to a group-normalized score in GRPO (Shao et al., 2024) and the Generalized Advantage Estimator (Schulman et al., 2015b) in PPO (Schulman et al., 2017). The clipping function

$\text{clip}(\cdot)$ constrains the likelihood ratio, thereby preventing excessively large policy updates and ensuring training stability. Without loss of generality, we adopt the generalized clipping formulation proposed by (Wang et al., 2019):

$$\text{clip}^{\text{ratio}}(w_t(\theta), l_t, u_t) = \begin{cases} w_t(\theta), & l_t \leq w_t(\theta) \leq u_t \\ l_t, & w_t(\theta) \leq l_t \\ u_t, & w_t(\theta) \geq u_t \end{cases} \quad (3)$$

where l_t and u_t denote the lower and upper clipping ranges, respectively. PPO and GRPO both use the symmetric clipping ranges ($l_t = 1 - \epsilon$, $u_t = 1 + \epsilon$), while DAPO (Yu et al., 2025) uses the asymmetric clipping ranges ($l_t = 1 - \epsilon_l$, $u_t = 1 + \epsilon_u$).

Despite the popularity of ratio-based clipping, Wang et al. identified a mismatch between the ratio-based and the KL-based constraints, and accordingly proposed an alternative KL-based clipping function:

$$\text{clip}^{\text{KL}}(w_t(\theta), \delta) = \begin{cases} w_t(\theta), & \text{KL}_t(\theta) \leq \delta, \\ w_t(\theta_{\text{old}}), & \text{otherwise,} \end{cases} \quad (4)$$

where δ is the trust-region threshold and $\text{KL}_t(\theta) \triangleq \text{KL}_t(\pi_{\theta}(\cdot|s_t) || \pi_{\theta_{\text{old}}}(\cdot|s_t))$ involves an expectation over the full action space (Eq. (2)). We distinguish loss functions induced by different clipping functions using subscripts. For instance, the objectives corresponding to ratio-based and KL-based clipping are denoted by $\mathcal{L}^{\text{ratio}}$ and \mathcal{L}^{KL} , respectively.

4. Method

4.1. A Unified Clipping Framework

We first propose a unified framework that subsumes both ratio-based and KL-based policy constraints, while naturally accommodating more general constraint variants. Specifically, we define a general clipping operator as

$$\text{clip}_{\text{general}}(w_t(\theta), \mathcal{C}) = \begin{cases} w_t(\theta), & \text{if } \mathcal{C}_t(\theta) \text{ is true} \\ w_t(\theta_{\text{old}}), & \text{otherwise} \end{cases} \quad (5)$$

where the constraint function $\mathcal{C}_t(\theta)$ encodes a prescribed feasibility condition on the policy corresponding to the sample (s_t, a_t) . This formulation provides a flexible abstraction

of policy divergence constraints: rather than committing to a specific measure, the operator admits arbitrary constraint functions that define how policy divergences are measured and restricted at the sample level.

Under this unified clipping framework, existing methods can be recovered as special cases by specifying different choices of the constraint function, as illustrated in Table 1. In particular, when the constraint is set as $\mathcal{C}_t^{\text{KL}}(\theta) := \text{KL}_t(\theta) \leq \delta$, the resulting surrogate objective exactly recovers the original KL-constrained formulation, i.e., $\mathcal{L}_{\text{general}}^{\text{KL}}(\theta) = \mathcal{L}^{\text{KL}}(\theta)$, corresponding to an explicit trust-region constraint. When the constraint is set as $\mathcal{C}_t^{\text{ratio}}(\theta) := l_t \leq w_t \leq u_t$, the resulting surrogate objective yields the same gradient as the standard ratio-based clipping objective. As a result, this choice implicitly constrains policy updates without explicitly enforcing a trust-region constraint. We formalize this equivalence in the following theorem.

Theorem 4.1 (Gradient Equivalence). Let the constraint be defined as $\mathcal{C}_t^{\text{ratio}}(\theta) := l_t \leq w_t(\theta) \leq u_t$. Then, for any parameter θ where the objective is differentiable, the gradient of the general objective is equivalent to that of the ratio-based objective: $\nabla \mathcal{L}^{\text{ratio}}(\theta) = \nabla \mathcal{L}_{\text{general}}^{\text{ratio}}(\theta)$.

4.2. Analysis of KL3 Estimator and ATR-GRPO

We have shown that both ratio-based and KL-based objectives are special cases of the unified formulation in Eq. (5). Next, we investigate other policy divergence constraints that can be incorporated within this framework. Previous literature has shown that the KL-based constraint $\text{KL}(\theta) \leq \delta$ aligns with the original trust-region theory, which enforces monotonic policy improvement (Schulman et al., 2015a; Wang et al., 2020; 2019). However, in the context of LLMs, enforcing such a KL-based constraint is often intractable, as it requires computing the full expectation of the KL divergence over an extremely large action space.

To address this limitation, Schulman proposed several Monte-Carlo estimators to approximate the KL divergence. Among them, the most widely used estimator is the KL3_t operator, which admits a lightweight surrogate expression:

$$\text{KL3}_t(\theta) := w_t(\theta) - 1 - \log w_t(\theta). \quad (6)$$

This estimator offers several appealing properties. First, it can be computed at the sample level without requiring an explicit expectation over the entire action space, which is crucial for large-scale policies such as LLMs. Second, KL3_t is non-negative and exhibits substantially lower variance than naive Monte-Carlo KL estimators. Finally, KL3_t provides a local approximation to the KL divergence near the identity ratio, and thus serves as a principled trust-region surrogate (Schulman, 2020).

Below, we analyze the relationship between different policy divergence constraints within the unified framework. As

implied by Eq. (6), $\text{KL3}_t(\theta)$ can be viewed as a function of the ratio $w_t(\theta)$, and we show that the two constraints (likelihood ratio and KL divergence) are equivalent under appropriate hyperparameter choices.

Theorem 4.2 (Equivalence and Asymmetry). Define lower and upper clipping ranges for a given threshold $\delta > 0$ as:

$$l_{\delta}^{\text{KL3}} = \min_{\theta} w_t(\theta) \quad \text{s.t.} \quad \text{KL3}_t(\theta) \leq \delta,$$

$$u_{\delta}^{\text{KL3}} = \max_{\theta} w_t(\theta) \quad \text{s.t.} \quad \text{KL3}_t(\theta) \leq \delta.$$

- (1) The constraint $\text{KL3}_t(\theta) \leq \delta$ is equivalent to $l_{\delta}^{\text{KL3}} \leq w_t(\theta) \leq u_{\delta}^{\text{KL3}}$, where $0 < l_{\delta}^{\text{KL3}} < 1 < u_{\delta}^{\text{KL3}}$.
- (2) These ranges satisfy the asymmetry property: $1 - l_{\delta}^{\text{KL3}} < u_{\delta}^{\text{KL3}} - 1$.

The proof of Theorem 4.2 is provided in Appendix A.1. Theorem 4.2 reveals an explicit connection between the KL3-based and ratio-based constraints by characterizing the admissible likelihood ratio ranges under the KL3 constraint, in the spirit of TRGPO (Wang et al., 2019). **Importantly, our goal here is to reveal this underlying relationship between these two types of constraints, instead of how to compute these clipping ranges explicitly.** In practice, it is not necessary to explicitly compute the clipping ranges, but can directly restrict policy divergences through the specified clipping function $\mathcal{C}_t(\theta)$ in Eq. (5).

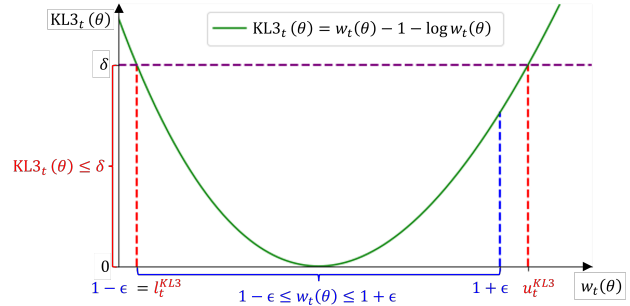


Figure 1. Illustration of the KL3-based constraint.

As implied by Theorem 4.2 (1), the KL3-based constraint is equivalent to a ratio-based constraint with a specific choice of hyperparameters. Furthermore, as implied by Theorem 4.2 (2), the KL3-based constraint always induces an asymmetric clipping range, where the upper clipping range deviates more than the lower range does ($1 - l_{\delta}^{\text{KL3}} < u_{\delta}^{\text{KL3}} - 1$). Also, as illustrated in the Figure 1, the constraint $\text{KL3}_t(\theta) \leq \delta$ results in a larger upper clipping range compared to the symmetric clipping range $(1 - \epsilon, 1 + \epsilon)$, where we set $\epsilon = 1 - l_{\delta}^{\text{KL3}}$. This property is consistent with prior work, such as Clip-Higher (Yu et al., 2025). However, unlike heuristic asymmetric clipping rules of Clip-Higher, the KL3-based constraint provides an exact and principled

characterization of this asymmetry, thereby offering a theoretically grounded mechanism for tuning the clipping range.

Building upon these observations, we formally propose Approximate Trust Region-based GRPO (ATR-GRPO), which integrates the KL3 constraint directly into the unified framework (Eq. (5)) by setting $\mathcal{C}_t(\theta) := \text{KL3}_t(\theta) \leq \delta$. Different from GRPO, ATR-GRPO enforces the approximate trust-region constraint through the ATR-based clipping ($w_t(\theta) \in [l_\delta^{\text{KL3}}, u_\delta^{\text{KL3}}]$) within the unified framework (Eq. (5)), enabling stable policy updates without explicitly computing the full KL expectations.

5. Theoretical Analysis

In this section, we present a comprehensive theoretical analysis of ATR-based clipping and ratio-based clipping, building on the frameworks developed in prior works (Cui et al., 2025; Park et al., 2025). We formally characterize the induced policy logit differences (Theorem 5.1) and analyze their impact on policy entropy difference (Theorem 5.2).

5.1. Setup and Assumptions

We assume that GRPO (symmetric ratio-based clipping) and ATR-GRPO (ATR-based clipping) both utilize the full-batch gradients under the standard policy gradient algorithm (Williams, 1992). Furthermore, the policy π_θ is modeled as a softmax policy $\pi_\theta(a|s) = \frac{\exp(\theta_{s,a})}{\sum_{a' \in \mathcal{A}(s)} \exp(\theta_{s,a'})}$. We mainly consider two representative cases, and we denote the corresponding probabilistic events as:

$$X_-(s) := \{a \in \mathcal{A}(s) | w_t(\theta_{s,a}) \in [1 - \epsilon, l_\delta^{\text{KL3}}], 1 + \epsilon = u_\delta^{\text{KL3}}\},$$

$$X_+(s) := \{a \in \mathcal{A}(s) | w_t(\theta_{s,a}) \in [1 + \epsilon, u_\delta^{\text{KL3}}], 1 - \epsilon = l_\delta^{\text{KL3}}\},$$

where $X_-(s)$ and $X_+(s)$ represent the event of unsatisfying and satisfying the KL3 constraint (approximate trust-region constraint), respectively. We define $\mathbb{I}_{X_-(s)}(a)$ and $\mathbb{I}_{X_+(s)}(a)$ to be the indicator function for $X_-(s)$ and $X_+(s)$, respectively.

5.2. Policy Logits Difference Analysis

Let $\theta_{s,a}^k$ denote the policy logits at the k -th step. We denote the updated policy logits for the ratio-based and ATR-based clipping methods as $\theta_{s,a}^{\text{ratio},k+1}$ and $\theta_{s,a}^{\text{ATR},k+1}$, respectively. We define $\Delta\theta_{s,a} := \theta_{s,a}^{\text{ATR},k+1} - \theta_{s,a}^{\text{ratio},k+1}$ as the policy logits difference between ATR-based clipping and the ratio-based clipping. We characterize $\Delta\theta_{s,a}$ under different events in the following Theorem 5.1 and provide proof in Appendix A.2.

Theorem 5.1 (Policy Logits Difference). Consider the policy gradient algorithm with learning rate η and given the state visitation distribution $d^{\pi_{\theta_{\text{old}}}(s)}$ induced by $\pi_{\theta_{\text{old}}}$. Let $\Delta\theta_{s,a}$ denote the policy logits difference between the ATR-based

and ratio-based clipping methods.

Under event $X_-(s)$, we have

$$\Delta\theta_{s,a} = -\eta d^{\pi_{\theta_{\text{old}}}(s)} \pi_{\theta^k}(a|s) \left[A \mathbb{I}_{X_-(s)}(a) \right. \\ \left. - \mathbb{E}_{a' \sim \pi_{\theta^k}(\cdot|s)} [A \mathbb{I}_{X_-(s)}(a')] \right].$$

Under event $X_+(s)$, we have

$$\Delta\theta_{s,a} = \eta d^{\pi_{\theta_{\text{old}}}(s)} \pi_{\theta^k}(a|s) \left[A \mathbb{I}_{X_+(s)}(a) \right. \\ \left. - \mathbb{E}_{a' \sim \pi_{\theta^k}(\cdot|s)} [A \mathbb{I}_{X_+(s)}(a')] \right].$$

5.3. Entropy Difference Analysis

Building upon Theorem 5.1, we characterize the exploration behaviours of ATR-based clipping by deriving the entropy difference $\Delta\mathcal{H} := \mathcal{H}(\theta^{\text{ATR},k+1}|s) - \mathcal{H}(\theta^{\text{ratio},k+1}|s)$ in the following theorem. The proof is provided in Appendix A.3.

Theorem 5.2 (Entropy Difference). The entropy difference $\Delta\mathcal{H}$ between the ATR-based and ratio-based clipping methods is related to the covariance between the advantage and the log-likelihood.

Under event $X_-(s)$, we have

$$\Delta\mathcal{H} = \eta d^{\pi_{\theta_{\text{old}}}(s)} \text{Cov}_{a \sim \pi_{\theta^k}(\cdot|s)} (A \mathbb{I}_{X_-(s)}(a), \log \pi_{\theta^k}(a|s)).$$

Under event $X_+(s)$, we have

$$\Delta\mathcal{H} = -\eta d^{\pi_{\theta_{\text{old}}}(s)} \text{Cov}_{a \sim \pi_{\theta^k}(\cdot|s)} (A \mathbb{I}_{X_+(s)}(a), \log \pi_{\theta^k}(a|s)).$$

Theorem 5.2 implies that the entropy difference depends on the covariance between the advantage under the specific event and the log-likelihood of π_{θ^k} . Crucially, this dependency reveals that ATR-based clipping exhibits exploration behavior that is better aligned with the approximate trust-region constraint than ratio-based clipping. We identify this as the dynamic exploration mechanism: **it enforces conservative exploration when updates are large and potentially risky ($X_-(s)$) while permitting expansive exploration when updates are within the approximate trust-region ($X_+(s)$)**.

Specifically, when the approximate trust-region constraint is unsatisfied ($X_-(s)$), ATR-based clipping maintains higher entropy than ratio-based clipping when there is an alignment between the advantage and policy likelihood (i.e., advantageous and high-probability actions). By preserving entropy in these high-confidence regions, our ATR-based clipping method prioritizes stability, anchoring the policy to high-confidence actions, preventing the premature amplification of low-confidence tails that lead to instability.

Table 2. Performance comparison on the AMC2023, AIME2024, and AIME2025 benchmarks. We report both the final and best evaluation performance (formatted as final (best)). The best performance is highlighted.

Method	AMC2023		AIME2024		AIME2025		Average	
	Mean@8 (%)	Pass@8 (%)						
Qwen3-1.7B								
Base Model	28.61	48.19	6.67	13.33	4.17	20.00	13.15	27.18
Clip	40.21 (40.21)	60.24 (67.47)	10.00 (10.00)	23.33 (26.67)	10.42 (12.50)	20.00 (26.67)	20.21 (20.41)	34.52 (36.93)
Clip-Higher	37.65 (37.80)	66.27 (66.27)	10.42 (10.83)	23.33 (30.00)	6.25 (10.42)	16.67 (26.67)	18.11 (18.68)	35.42 (37.15)
Dual Clip	42.02 (42.02)	65.06 (68.67)	10.83 (11.67)	30.00 (33.33)	12.50 (13.33)	23.33 (26.67)	21.78 (21.78)	39.46 (39.56)
Dynamic Clipping	41.72 (41.72)	63.86 (67.47)	9.17 (11.67)	20.00 (30.00)	11.67 (12.92)	23.33 (26.67)	20.85 (21.56)	35.73 (38.35)
Clip-Cov	33.58 (36.14)	61.45 (67.47)	7.92 (9.58)	20.00 (23.33)	7.50 (10.83)	16.67 (23.33)	16.33 (18.80)	32.70 (34.93)
Soft Gate	42.92 (42.92)	68.67 (68.67)	8.33 (9.58)	26.67 (30.00)	13.33 (13.33)	23.33 (26.67)	21.53 (21.53)	39.56 (39.87)
ATR-based Clipping (ours)	41.72 (45.03)	69.88 (72.29)	13.33 (13.33)	26.67 (36.67)	13.75 (14.58)	30.00 (30.00)	22.93 (23.07)	42.18 (44.00)
Qwen3-8B								
Base Model	26.05	50.60	5.42	16.67	1.25	6.67	10.91	24.65
Clip	45.78 (48.34)	72.29 (74.70)	12.92 (18.33)	26.67 (36.67)	15.83 (15.83)	30.00 (33.33)	24.84 (26.81)	42.99 (46.01)
Clip-Higher	53.77 (56.33)	73.49 (78.31)	20.83 (24.17)	43.33 (46.67)	19.58 (21.67)	26.67 (30.00)	31.39 (33.36)	47.83 (51.66)
Dual Clip	55.57 (55.72)	77.11 (78.31)	21.25 (24.17)	36.67 (46.67)	19.58 (22.50)	26.67 (33.33)	32.14 (33.34)	46.81 (49.75)
Dynamic Clipping	53.16 (54.97)	78.31 (78.31)	23.75 (24.58)	50.00 (50.00)	20.83 (22.92)	33.33 (36.67)	32.58 (32.93)	53.88 (53.88)
Clip-Cov	50.75 (55.12)	69.88 (75.90)	21.25 (22.50)	46.67 (46.67)	20.83 (22.08)	33.33 (33.33)	30.95 (32.48)	49.96 (50.05)
Soft Gate	53.01 (53.01)	74.70 (74.70)	20.42 (22.92)	43.33 (43.33)	19.17 (19.17)	26.67 (30.00)	30.87 (31.17)	48.23 (48.23)
ATR-based Clipping (ours)	56.02 (56.02)	80.72 (80.72)	25.42 (25.83)	50.00 (50.00)	19.58 (22.92)	30.00 (36.67)	33.67 (33.67)	53.57 (53.57)

Conversely, when the approximate trust-region constraint is satisfied ($X_+(s)$), our method increases entropy when there is a misalignment between the advantage and policy likelihood (i.e., advantageous yet low-probability actions). This regime drives aggressive exploration, actively reallocating probability mass toward promising but underexplored parts of the action space, improving efficiency without compromising the approximate trust-region constraints.

6. Experiments

6.1. Experiment Setting

We implement all experiments using the Un-sloth (Daniel Han & team, 2023) and TRL (von Werra et al., 2020) frameworks. We fine-tune the Qwen3-1.7B and Qwen3-8B models (Yang et al., 2025a) on the DAPO-Math-17k dataset (Yu et al., 2025), employing a sparse binary reward function, where the model receives a reward of +1 upon generating the correct final answer, and 0 otherwise. To mitigate computational overhead, we employ Low-Rank Adaptation (LoRA) (Schulman & Lab, 2025), which injects low-rank adapter matrices to optimize a minimal set of parameters, greatly reducing memory requirements without compromising performance (Schulman & Lab, 2025).

We compare our approach against SOTA clipping methods, including Clip-Higher (Yu et al., 2025), Dynamic Clipping (Yang et al., 2025b), Clip-Cov (Cui et al., 2025), and Soft Gate (Gao et al., 2025). To ensure a fair comparison, we standardize Dr.GRPO (Liu et al., 2025c) as the backbone RL algorithm across all baselines, varying only the clipping mechanism. Consistent with this setup, we denote our method (ATR-GRPO) as ATR-based clipping in the exper-

iments to explicitly highlight our primary distinction. We train each method for 1,000 gradient steps, evaluating performance every 50 steps on the AMC2023 (Li et al., 2024), AIME2024 (Veeraboina, 2023), and AIME2025 (AIME, 2025) benchmarks. The implementation details are provided in Appendix B. The full codebase used to reproduce our experimental results is included in the supplementary material.

6.2. Performance Comparison

As shown in Table 2, we conduct a comprehensive evaluation of the proposed ATR-based clipping method against SOTA baselines on the AMC2023, AIME2024, and AIME2025 benchmarks. We evaluate the performance of both Qwen3-1.7B and Qwen3-8B using Mean@8 and Pass@8. Mean@8 measures the average accuracy across 8 sampled responses, while Pass@8 indicates the success rate where at least one of the 8 samples is correct. We primarily report the evaluation performance of the **final** checkpoint, and additionally present the **best** evaluation performance achieved during training.

Performance on Qwen3-1.7B. Our proposed method achieves substantial improvements over the base model and consistently outperforms existing baselines on Qwen3-1.7B. Specifically, our method achieves the highest scores on the **final** evaluation performance (Average), with the Mean@8 of 22.93% and Pass@8 of 42.18%, surpassing the best baseline (Dual Clip). Specifically, for challenging AIME2025, our method achieves the **final** Mean@8 of 13.75% compared to 13.33% for Soft Gate, the best baseline.

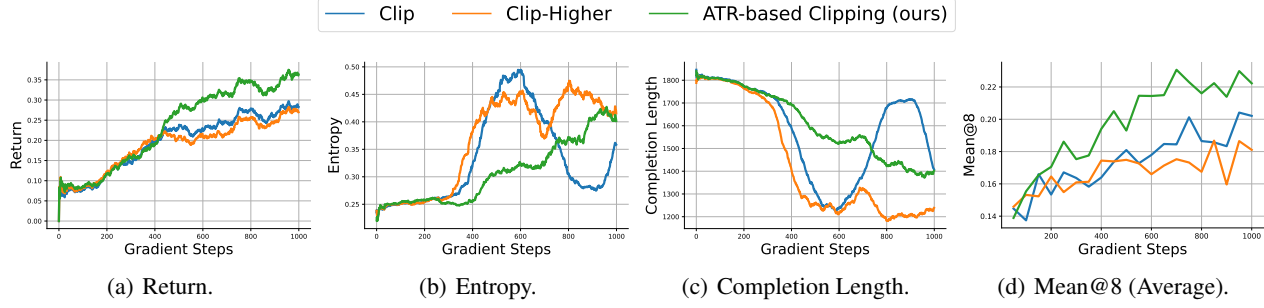


Figure 2. Comparison of Clip, Clip-Higher, and ATR-based clipping on Qwen3-1.7B. The training curves for (a) return, (b) entropy, and (c) completion length are smoothed with a 100-step moving average window. (d) Evaluation performance of Mean@8 (Average).

Performance on Qwen3-8B. Our method continues to exhibit superior performance on Qwen3-8B, particularly on the AMC2023 and AIME2024. On AMC2023, our method achieves a **final** Mean@8 of 56.02% and Pass@8 of 80.72%. Furthermore, on AIME2024, our approach demonstrates superior robustness, achieving a **final** Mean@8 of 25.42% and Pass@8 of 50.00%, outperforming Dynamic Clipping. While Dynamic Clipping proves competitive on AIME2025, our method yields the highest **final** Mean@8 of 33.67% (Average).

6.3. Efficiency and Stability Analysis

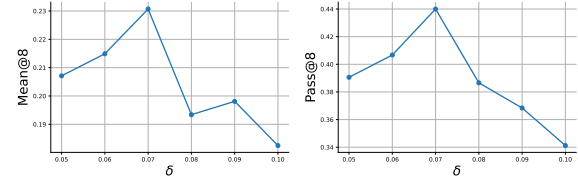
We now analyze the learning stability and efficiency of ATR-based clipping, comparing it primarily against the Clip and Clip Higher methods, the two baselines most closely related to and as computationally simple as ours. We present the training curves for return, entropy and completion length alongside evaluation performance (Mean@8) in Figure 2.

Specifically, as shown in Figure 2(a), while the returns of all methods are initially similar, ATR-based clipping surpasses the baselines around 400 gradient steps, continuing to improve to the return of 0.36, whereas the baselines both plateau near 0.28, demonstrating that our modification yields efficient performance improvements. This trend is mirrored in the evaluation tasks (Figure 2(d)), where our method consistently outperforms baselines, confirming the superior sample efficiency of ATR-based clipping.

Moreover, our method does not sacrifice the learning stability. As presented in Figure 2(b), unlike the Clip method, ATR-based clipping maintains a steady, moderate entropy level, indicating a stable exploration strategy that avoids premature convergence or policy collapse. In terms of the completion length (Figure 2(c)), ATR-based clipping exhibits a stable, monotonic decrease. In contrast, the baselines show erratic oscillations (Clip) or sharp, potentially premature drops (Clip-Higher), showing our proposed method effectively stabilizes the learning process.

6.4. Ablation Studies

Trust Region Threshold δ . Specifically, we show Mean@8 and Pass@8 with varying δ in Figure 3(a) and Figure 3(b), respectively. Both metrics exhibit a similar trend, steadily increasing from $\delta = 0.05$ and peaking at $\delta = 0.07$. However, further increasing δ results in sharp performance degeneration. The results indicate that an overly small δ imposes stronger constraints that hinder performance improvement, while an excessively large δ leads to training instability or policy collapse, thereby degrading performance.



(a) Mean@8 with varying δ . (b) Pass@8 with varying δ .

Figure 3. Ablation experiments of ATR-GRPO on Qwen3-1.7B. The performance for (a) Mean@8 and (b) Pass@8 with varying δ .

Fine-grained Tuning Clip and Clip-Higher. To ensure that our performance gains stem from fundamental algorithmic improvements rather than sub-optimal baseline configurations, we conducted extensive hyperparameter tuning on **Clip** and **Clip-Higher** baselines. Specifically, we evaluated **Clip** with $\epsilon \in \{0.1, 0.2, 0.3, 0.4, 0.5\}$, reporting the performance achieved by the optimal configuration. Additionally, for the trust region threshold $\delta = 0.07$, we have corresponding ATR-based clipping range of $[l_{\delta}^{\text{KL3}}, u_{\delta}^{\text{KL3}}] = [0.671, 1.422]$. We specifically configured Clip and Clip-Higher using these two ranges, including **Clip** ($\epsilon \in \{0.329, 0.422\}$) and **Clip-Higher** ($\epsilon_l = 0.329$, $\epsilon_u \in \{0.5, 0.6\}$). As shown in Table 3, our method achieves the highest performance of Mean@8 and Pass@8 (Average) compared to these meticulously tuned baselines.

Table 3. Performance comparison on Qwen3-1.7B across various KL estimators and fine-grained hyperparameter configurations for Clip and Clip-Higher. Each method is independently trained using 3 separate runs. We report the mean and standard deviation of the performance based on the final checkpoints from these 3 runs. The best performance is highlighted.

Method	Qwen3-1.7B							
	AMC2023		AIME2024		AIME2025		Average	
	Mean@8 (%)	Pass@8 (%)						
Clip ($\epsilon = 0.2$)	39.81 \pm 0.26	61.45 \pm 2.60	8.47 \pm 0.86	26.67 \pm 0.00	10.97 \pm 0.39	22.22 \pm 1.57	19.75 \pm 0.10	36.78 \pm 1.27
Clip ($\epsilon \in \{0.1, 0.2, 0.3, 0.4, 0.5\}$)	41.97 \pm 0.14	65.86 \pm 1.50	11.67 \pm 1.02	27.78 \pm 4.16	14.17 \pm 1.23	28.89 \pm 1.57	22.60 \pm 0.63	40.84 \pm 1.53
Clip ($\epsilon = 0.329$)	40.18 \pm 1.60	64.26 \pm 3.98	11.81 \pm 1.87	32.22 \pm 1.57	11.25 \pm 0.68	22.22 \pm 1.57	21.07 \pm 0.95	39.57 \pm 2.33
Clip ($\epsilon = 0.422$)	40.16 \pm 0.14	63.05 \pm 2.27	8.61 \pm 1.19	24.44 \pm 3.14	10.14 \pm 0.39	23.33 \pm 0.00	19.64 \pm 0.38	36.94 \pm 0.29
Clip-Higher ($\epsilon_l = 0.2, \epsilon_u = 0.28$)	36.75 \pm 0.56	64.66 \pm 3.16	9.17 \pm 0.59	21.11 \pm 1.57	8.47 \pm 0.86	20.00 \pm 2.72	18.13 \pm 0.64	35.26 \pm 2.10
Clip-Higher ($\epsilon_l = 0.329, \epsilon_u = 0.5$)	39.66 \pm 0.61	61.85 \pm 2.05	7.64 \pm 0.39	22.22 \pm 3.14	11.81 \pm 0.20	23.33 \pm 2.72	19.70 \pm 0.24	35.80 \pm 2.31
Clip-Higher ($\epsilon_l = 0.329, \epsilon_u = 0.6$)	42.72 \pm 0.68	66.67 \pm 1.50	10.83 \pm 0.34	27.78 \pm 1.57	12.22 \pm 0.39	23.33 \pm 2.72	21.93 \pm 0.21	39.26 \pm 0.60
KL1 ($\delta = 0.07$)	41.47 \pm 1.40	65.86 \pm 2.27	8.19 \pm 0.20	24.44 \pm 3.14	12.78 \pm 1.19	24.44 \pm 5.67	20.81 \pm 0.77	38.25 \pm 3.67
KL2 ($\delta = 0.07$)	43.22 \pm 1.23	67.07 \pm 1.14	11.11 \pm 1.37	26.67 \pm 2.72	13.33 \pm 0.90	24.44 \pm 3.14	22.56 \pm 0.66	39.39 \pm 1.75
Full KL-Guided Clipping ($\delta = 0.07$) (Wang et al., 2019)	38.70 \pm 0.44	62.65 \pm 0.98	8.47 \pm 1.37	23.33 \pm 2.72	10.14 \pm 0.86	21.11 \pm 1.57	19.11 \pm 0.65	35.70 \pm 0.29
IS-weighted KL3 ($\delta = 0.07$)	39.26 \pm 0.40	64.66 \pm 1.50	8.75 \pm 1.48	26.67 \pm 4.71	11.67 \pm 0.68	24.44 \pm 1.57	19.89 \pm 0.38	38.59 \pm 1.98
KL3 ($\delta = 0.07, l_\delta^{\text{KL3}} = 0.671, u_\delta^{\text{KL3}} = 1.422$)	43.17 \pm 1.17	68.67 \pm 0.98	13.06 \pm 1.71	27.78 \pm 4.16	14.03 \pm 1.71	28.89 \pm 1.57	23.42 \pm 1.04	41.78 \pm 2.00

Crucially, our method outperforms Clip ($\epsilon = 0.329$ and $\epsilon = 0.422$), validating our previous statement and theoretical analysis (Theorem 5.2).

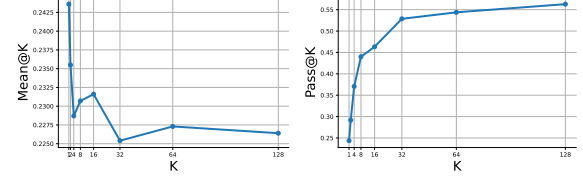
KL Estimators. Furthermore, we evaluate alternative KL estimators (KL1, KL2, Full KL-guided clipping, and IS-weighted KL3) under the same trust region threshold ($\delta = 0.07$), as presented in Table 3. The results demonstrate that KL3 consistently yields the performance gains. While recent studies (Shah et al., 2025; Liu et al., 2025b; Zhang et al., 2025b; Liu et al., 2025a) have explored KL estimators primarily as loss regularization terms or auxiliary reward signals, we investigate a different application, utilizing the KL estimator to guide the clipping criterion. We empirically demonstrate that KL3 is the best choice among these KL estimators for this specific purpose.

Test-time Sample Budget. Then, we further report Mean@K (Figure 4(a)) and Pass@K (Figure 4(b)) for ATR-GRPO on Qwen3-1.7B with varying K. As K increases, Mean@K remains stable around 0.23. In contrast, Pass@K exhibits an increasing trend, scaling with the test-time sample budget from 24.36% at Pass@1 to 56.29% at Pass@128.

6.5. Limitations and Future Works

Adaptive Trust Region Threshold. Employing a static trust region threshold throughout the entire training process may be suboptimal. Inspired by existing works (Wang et al., 2019; Yang et al., 2025b), we will investigate mechanisms to adaptively adjust δ based on the policy probability and entropy for more stable and efficient learning in the future.

Sequence-level Integration. While this work primarily focuses on the token-level objective, we recognize the limitation posed by the mismatch between token-level importance sampling and sequence-level rewards, leading to high-variance gradients and unstable training (Zheng et al.,



(a) Mean@K with varying K. (b) Pass@K with varying K.

Figure 4. The performance (Average) of ATR-GRPO on Qwen3-1.7B for (a) Mean@K and (b) Pass@K with varying K.

2025). We aim to explore the extension of our framework to sequence-level objectives in future work.

7. Conclusion

In this work, we introduce a unified clipping framework for policy optimization that generalizes the notion of policy divergence, encompassing both ratio-based and KL-based constraints. From this foundational perspective, we analyze and identify the KL3 estimator as a particularly effective policy divergence measure. Based on this insight, we proposed ATR-GRPO that actively reallocates probability mass toward promising actions rather than passively truncating updates through ratio-based clipping. Our theoretical analysis demonstrates that ATR-GRPO enables more principled and effective exploration than standard symmetric ratio-based clipping, while preserving the computational efficiency of GRPO. Empirically, comprehensive experiments across multiple verifiable mathematical reasoning benchmarks demonstrate that ATR-GRPO yields performance improvements in both training stability and final performance compared to existing baselines. These results underscore the central role of the policy divergence constraint in policy optimization and suggest that exploring alternative policy divergence measures is a promising direction for advancing LLMs.

References

Ahmadian, A., Cremer, C., Gallé, M., Fadaee, M., Kreutzer, J., Pietquin, O., Üstün, A., and Hooker, S. Back to basics: Revisiting reinforce style optimization for learning from human feedback in llms. *arXiv preprint arXiv:2402.14740*, 2024.

AIME. AIME Problems and Solutions, 2025. URL https://artofproblemsolving.com/wiki/index.php/AIME_Problems_and_Solutions.

Berner, C., Brockman, G., Chan, B., Cheung, V., Debiak, P., Dennison, C., Farhi, D., Fischer, Q., Hashme, S., Hesse, C., et al. Dota 2 with large scale deep reinforcement learning. *arXiv preprint arXiv:1912.06680*, 2019.

Chiang, W.-L., Zheng, L., Sheng, Y., Angelopoulos, A. N., Li, T., Li, D., Zhu, B., Zhang, H., Jordan, M., Gonzalez, J. E., et al. Chatbot arena: An open platform for evaluating llms by human preference. In *Forty-first International Conference on Machine Learning*, 2024.

Cobbe, K., Kosaraju, V., Bavarian, M., Chen, M., Jun, H., Kaiser, L., Plappert, M., Tworek, J., Hilton, J., Nakano, R., et al. Training verifiers to solve math word problems. *arXiv preprint arXiv:2110.14168*, 2021.

Cui, G., Zhang, Y., Chen, J., Yuan, L., Wang, Z., Zuo, Y., Li, H., Fan, Y., Chen, H., Chen, W., et al. The entropy mechanism of reinforcement learning for reasoning language models. *arXiv preprint arXiv:2505.22617*, 2025.

Daniel Han, M. H. and team, U. Unslloth, 2023. URL <http://github.com/unslothai/unslloth>.

Gao, C., Zheng, C., Chen, X.-H., Dang, K., Liu, S., Yu, B., Yang, A., Bai, S., Zhou, J., and Lin, J. Soft adaptive policy optimization. *arXiv preprint arXiv:2511.20347*, 2025.

Hu, J., Zhang, Y., Han, Q., Jiang, D., Zhang, X., and Shum, H.-Y. Open-reasoner-zero: An open source approach to scaling up reinforcement learning on the base model. *arXiv preprint arXiv:2503.24290*, 2025.

Jain, N., Han, K., Gu, A., Li, W.-D., Yan, F., Zhang, T., Wang, S., Solar-Lezama, A., Sen, K., and Stoica, I. Livecodebench: Holistic and contamination free evaluation of large language models for code. *arXiv preprint arXiv:2403.07974*, 2024.

Kaelbling, L. P., Littman, M. L., and Moore, A. W. Reinforcement learning: A survey. *Journal of artificial intelligence research*, 4:237–285, 1996.

Kakade, S. M. A natural policy gradient. *Advances in neural information processing systems*, 14, 2001.

Lambert, N., Morrison, J., Pyatkin, V., Huang, S., Ivison, H., Brahman, F., Miranda, L. J. V., Liu, A., Dziri, N., Lyu, S., et al. Tulu 3: Pushing frontiers in open language model post-training. *arXiv preprint arXiv:2411.15124*, 2024.

Li, J., Beeching, E., Tunstall, L., Lipkin, B., Soletskyi, R., Huang, S., Rasul, K., Yu, L., Jiang, A. Q., Shen, Z., et al. Numinamath: The largest public dataset in ai4maths with 860k pairs of competition math problems and solutions. *Hugging Face repository*, 13(9):9, 2024.

Liu, A., Mei, A., Lin, B., Xue, B., Wang, B., Xu, B., Wu, B., Zhang, B., Lin, C., Dong, C., et al. Deepseek-v3. 2: Pushing the frontier of open large language models. *arXiv preprint arXiv:2512.02556*, 2025a.

Liu, K., Liu, J. K., Chen, M., and Liu, Y. Rethinking kl regularization in rlhf: From value estimation to gradient optimization. *arXiv preprint arXiv:2510.01555*, 2025b.

Liu, Z., Chen, C., Li, W., Qi, P., Pang, T., Du, C., Lee, W. S., and Lin, M. Understanding r1-zero-like training: A critical perspective. *arXiv preprint arXiv:2503.20783*, 2025c.

Loshchilov, I. and Hutter, F. Decoupled weight decay regularization. *arXiv preprint arXiv:1711.05101*, 2017.

Mnih, V., Kavukcuoglu, K., Silver, D., Graves, A., Antonoglou, I., Wierstra, D., and Riedmiller, M. Playing atari with deep reinforcement learning. *arXiv preprint arXiv:1312.5602*, 2013.

Moshkov, I., Hanley, D., Sorokin, I., Toshniwal, S., Henkel, C., Schifferer, B., Du, W., and Gitman, I. Aimo-2 winning solution: Building state-of-the-art mathematical reasoning models with openmathreasoning dataset. *arXiv preprint arXiv:2504.16891*, 2025.

Ouyang, L., Wu, J., Jiang, X., Almeida, D., Wainwright, C., Mishkin, P., Zhang, C., Agarwal, S., Slama, K., Ray, A., et al. Training language models to follow instructions with human feedback. *Advances in neural information processing systems*, 35:27730–27744, 2022.

Park, J. R., Kim, J., Kim, G., Jo, J., Choi, S., Cho, J., and Ryu, E. K. Clip-low increases entropy and clip-high decreases entropy in reinforcement learning of large language models. *arXiv preprint arXiv:2509.26114*, 2025.

Schulman, J. Approximating kl divergence, 2020. URL <http://joschu.net/blog/kl-approx.html>, 2020.

Schulman, J. and Lab, T. M. Lora without regret. *Thinking Machines Lab: Connectionism*, 2025. doi: 10.64434/tml.20250929. <https://thinkingmachines.ai/blog/lora/>.

Schulman, J., Levine, S., Abbeel, P., Jordan, M., and Moritz, P. Trust region policy optimization. In *International conference on machine learning*, pp. 1889–1897. PMLR, 2015a.

Schulman, J., Moritz, P., Levine, S., Jordan, M., and Abbeel, P. High-dimensional continuous control using generalized advantage estimation. *arXiv preprint arXiv:1506.02438*, 2015b.

Schulman, J., Wolski, F., Dhariwal, P., Radford, A., and Klimov, O. Proximal policy optimization algorithms. *arXiv preprint arXiv:1707.06347*, 2017.

Shah, V., Obando-Ceron, J., Jain, V., Bartoldson, B., Kailkhura, B., Mittal, S., Berseth, G., Castro, P. S., Bengio, Y., Malkin, N., et al. A comedy of estimators: On kl regularization in rl training of llms. *arXiv preprint arXiv:2512.21852*, 2025.

Shao, Z., Wang, P., Zhu, Q., Xu, R., Song, J., Bi, X., Zhang, H., Zhang, M., Li, Y., Wu, Y., et al. Deepseekmath: Pushing the limits of mathematical reasoning in open language models. *arXiv preprint arXiv:2402.03300*, 2024.

Sheng, G., Zhang, C., Ye, Z., Wu, X., Zhang, W., Zhang, R., Peng, Y., Lin, H., and Wu, C. Hybridflow: A flexible and efficient rlhf framework. In *Proceedings of the Twentieth European Conference on Computer Systems*, pp. 1279–1297, 2025.

Silver, D., Huang, A., Maddison, C. J., Guez, A., Sifre, L., Van Den Driessche, G., Schrittwieser, J., Antonoglou, I., Panneershelvam, V., Lanctot, M., et al. Mastering the game of go with deep neural networks and tree search. *nature*, 529(7587):484–489, 2016.

Sutton, R. S. and Barto, A. G. *Reinforcement learning: An introduction*. MIT press, 2018.

Tan, H., Pan, J., Lin, J., Chen, T., Zheng, Z., Tang, Z., and Yang, H. Gtpo and grp0-s: Token and sequence-level reward shaping with policy entropy. *arXiv preprint arXiv:2508.04349*, 2025.

Tesauro, G. Td-gammon, a self-teaching backgammon program, achieves master-level play. *Neural computation*, 6(2):215–219, 1994.

Veeraboina, H. Aime problem set 1983–2024, 2023. URL <https://www.kaggle.com/datasets/hemishveeraboina/aime-problem-set-1983-2024>.

von Werra, L., Belkada, Y., Tunstall, L., Beeching, E., Thrush, T., Lambert, N., Huang, S., Rasul, K., and Gallouédec, Q. Trl: Transformer reinforcement learning. <https://github.com/huggingface/trl>, 2020.

Wang, Y., He, H., Tan, X., and Gan, Y. Trust region-guided proximal policy optimization. *Advances in Neural Information Processing Systems*, 32, 2019.

Wang, Y., He, H., and Tan, X. Truly proximal policy optimization. In *Uncertainty in artificial intelligence*, pp. 113–122. PMLR, 2020.

Williams, R. J. Simple statistical gradient-following algorithms for connectionist reinforcement learning. *Machine learning*, 8(3):229–256, 1992.

Yang, A., Li, A., Yang, B., Zhang, B., Hui, B., Zheng, B., Yu, B., Gao, C., Huang, C., Lv, C., Zheng, C., Liu, D., Zhou, F., Huang, F., Hu, F., Ge, H., Wei, H., Lin, H., Tang, J., Yang, J., Tu, J., Zhang, J., Yang, J., Yang, J., Zhou, J., Zhou, J., Lin, J., Dang, K., Bao, K., Yang, K., Yu, L., Deng, L., Li, M., Xue, M., Li, M., Zhang, P., Wang, P., Zhu, Q., Men, R., Gao, R., Liu, S., Luo, S., Li, T., Tang, T., Yin, W., Ren, X., Wang, X., Zhang, X., Ren, X., Fan, Y., Su, Y., Zhang, Y., Zhang, Y., Wan, Y., Liu, Y., Wang, Z., Cui, Z., Zhang, Z., Zhou, Z., and Qiu, Z. Qwen3 technical report. *arXiv preprint arXiv:2505.09388*, 2025a.

Yang, S., Dou, C., Guo, P., Lu, K., Ju, Q., Deng, F., and Xin, R. Depo: Dynamic clipping policy optimization. *arXiv preprint arXiv:2509.02333*, 2025b.

Ye, D., Liu, Z., Sun, M., Shi, B., Zhao, P., Wu, H., Yu, H., Yang, S., Wu, X., Guo, Q., et al. Mastering complex control in moba games with deep reinforcement learning. In *Proceedings of the AAAI conference on artificial intelligence*, volume 34, pp. 6672–6679, 2020.

Yu, Q., Zhang, Z., Zhu, R., Yuan, Y., Zuo, X., Yue, Y., Dai, W., Fan, T., Liu, G., Liu, L., et al. Dapo: An open-source llm reinforcement learning system at scale. *arXiv preprint arXiv:2503.14476*, 2025.

Zhang, H., Da, J., Lee, D., Robinson, V., Wu, C., Song, W., Zhao, T., Raja, P., Zhuang, C., Slack, D., et al. A careful examination of large language model performance on grade school arithmetic. *Advances in Neural Information Processing Systems*, 37:46819–46836, 2024.

Zhang, Q., Wu, H., Zhang, C., Zhao, P., and Bian, Y. Right question is already half the answer: Fully unsupervised llm reasoning incentivization. *arXiv preprint arXiv:2504.05812*, 2025a.

Zhang, Y., Liu, Y., Yuan, H., Yuan, Y., Gu, Q., and Yao, A. C. On the design of kl-regularized policy gradient algorithms for llm reasoning. *arXiv preprint arXiv:2505.17508*, 2025b.

Zheng, C., Liu, S., Li, M., Chen, X.-H., Yu, B., Gao, C., Dang, K., Liu, Y., Men, R., Yang, A., et al. Group sequence policy optimization. *arXiv preprint arXiv:2507.18071*, 2025.

A. Proof Details

A.1. Equivalence and Asymmetry Analysis

Theorem A.1 (Equivalence and Asymmetry). Define the lower and upper clipping ranges for a given threshold $\delta > 0$ as:

$$l_{\delta}^{\text{KL3}} = \min_{\theta} w_t(\theta) \quad \text{s.t.} \quad \text{KL3}_t(\theta) \leq \delta,$$

$$u_{\delta}^{\text{KL3}} = \max_{\theta} w_t(\theta) \quad \text{s.t.} \quad \text{KL3}_t(\theta) \leq \delta.$$

(1) The constraint $\text{KL3}_t(\theta) \leq \delta$ is equivalent to $l_{\delta}^{\text{KL3}} \leq w_t(\theta) \leq u_{\delta}^{\text{KL3}}$, where $0 < l_{\delta}^{\text{KL3}} < 1 < u_{\delta}^{\text{KL3}}$.

(2) These ranges satisfy the asymmetry property: $1 - l_{\delta}^{\text{KL3}} < u_{\delta}^{\text{KL3}} - 1$.

Proof. For a given trust region threshold $\delta > 0$, we aim to find the area $(0 < l_{\delta}^{\text{KL3}} < 1 < u_{\delta}^{\text{KL3}})$ such that $\text{KL3}_t(\theta) \leq \delta, \forall w_t(\theta) \in [l_{\delta}^{\text{KL3}}, u_{\delta}^{\text{KL3}}]$.

Recall that

$$\text{KL3}_t(\theta) := w_t(\theta) - 1 - \log w_t(\theta) \quad (7)$$

We have

$$\begin{aligned} w_t(\theta) - 1 - \log w_t(\theta) &= \delta \\ \log w_t(\theta) &= w_t(\theta) - 1 - \delta \\ w_t(\theta) &= e^{w_t(\theta)-1-\delta} \\ w_t(\theta)e^{-w_t(\theta)} &= e^{-1-\delta} \\ -w_t(\theta)e^{-w_t(\theta)} &= -e^{-1-\delta} \end{aligned} \quad (8)$$

The Lambert W function is defined as $W(z)e^{W(z)} = z$. Then, let $w_t(\theta) = -W(z)$ and $z = -e^{-1-\delta}$, we have

$$w_t(\theta) = -W(-e^{-1-\delta}) \quad (9)$$

The equation has two real-valued Lambert solutions corresponding to the two real branches W_0 and W_{-1} for l_{δ}^{KL3} and u_{δ}^{KL3} , respectively. Specifically, we have

$$\begin{aligned} l_{\delta}^{\text{KL3}} &= -W_0(-e^{-1-\delta}) \in (0, 1) \\ u_{\delta}^{\text{KL3}} &= -W_{-1}(-e^{-1-\delta}) \in (1, +\infty) \end{aligned} \quad (10)$$

Then, we show that we always have $1 - l_{\delta}^{\text{KL3}} < u_{\delta}^{\text{KL3}} - 1$.

We have

$$\begin{aligned} \frac{d}{dw_t(\theta)} \text{KL3}_t(\theta) &= 1 - \frac{1}{w_t(\theta)}, \\ \frac{d^2}{d(w_t(\theta))^2} \text{KL3}_t(\theta) &= \frac{1}{(w_t(\theta))^2} > 0. \end{aligned} \quad (11)$$

Specifically, we have

$$\left| \frac{d}{dw_t(\theta)} \text{KL3}_t(\theta) \right| = \begin{cases} \frac{1}{w_t(\theta)} - 1, & w_t(\theta) < 1, \\ 1 - \frac{1}{w_t(\theta)}, & w_t(\theta) > 1, \end{cases} \quad (12)$$

We can observe that as $w_t(\theta) \rightarrow 0^+$, the slope magnitude $\left| \frac{d}{dw_t(\theta)} \text{KL3}_t(\theta) \right|$ diverges to infinity, whereas for $w_t(\theta) > 1$ it is uniformly bounded by 1. This implies that $\text{KL3}_t(w_t(\theta))$ increases more rapidly for $w_t(\theta) < 1$ than for $w_t(\theta) > 1$.

Recall that we have $l_\delta^{\text{KL3}} < 1 < u_\delta^{\text{KL3}}$. Since $\text{KL3}_t(\theta)$ is strictly convex on $(0, \infty)$ and satisfies $|\text{KL3}'_t(\theta)| \rightarrow \infty$ as $w_t(\theta) \rightarrow 0^+$ while $|\text{KL3}'_t(\theta)| < 1$ for $w_t(\theta) > 1$, the function grows faster for $w_t(\theta) < 1$ than for $w_t(\theta) > 1$. Therefore, to reach the same divergence level δ , the solution above 1 must deviate farther from 1 than the solution below 1, which implies that we always have

$$1 - l_\delta^{\text{KL3}} < u_\delta^{\text{KL3}} - 1. \quad (13)$$

□

A.2. Policy Logits Difference Analysis

Theorem A.2 (Policy Logits Difference). Consider the policy gradient algorithm with learning rate η and given the state visitation distribution $d^{\pi_{\theta_{\text{old}}}(s)}$ induced by $\pi_{\theta_{\text{old}}}$. Let $\Delta\theta_{s,a}$ denote the policy logits difference between the ATR-based and ratio-based clipping methods.

Under event $X_-(s)$, we have $\Delta\theta_{s,a} = -\eta d^{\pi_{\theta_{\text{old}}}(s)} \pi_{\theta^k}(a|s) \left[A \mathbb{I}_{X_-(s)}(a) - \mathbb{E}_{a' \sim \pi_{\theta^k}(\cdot|s)} [A \mathbb{I}_{X_-(s)}(a')] \right]$.

Under event $X_+(s)$, we have $\Delta\theta_{s,a} = \eta d^{\pi_{\theta_{\text{old}}}(s)} \pi_{\theta^k}(a|s) \left[A \mathbb{I}_{X_+(s)}(a) - \mathbb{E}_{a' \sim \pi_{\theta^k}(\cdot|s)} [A \mathbb{I}_{X_+(s)}(a')] \right]$.

Proof. Consider the clipped surrogate objective of ratio-based clipping:

$$\mathcal{J}^{\text{ratio}}(\theta) := \mathbb{E}_{\substack{y \sim \pi_{\theta_{\text{old}}}(\cdot|x) \\ x \sim D}} \left[\frac{1}{|y|} \sum_{t=1}^{|y|} \text{clip}^{\text{ratio}}(w_t(\theta), 1 - \epsilon, 1 + \epsilon) A_t \right]. \quad (14)$$

Consider the clipped surrogate objective of ATR-based clipping:

$$\mathcal{J}^{\text{ATR}}(\theta) := \mathbb{E}_{\substack{y \sim \pi_{\theta_{\text{old}}}(\cdot|x) \\ x \sim D}} \left[\frac{1}{|y|} \sum_{t=1}^{|y|} \text{clip}^{\text{ratio}}(w_t(\theta), l_\delta^{\text{KL3}}, u_\delta^{\text{KL3}}) A_t \right]. \quad (15)$$

Following the similar proof sketch of (Park et al., 2025), for a given trust region threshold δ and the corresponding ATR-based

clipping range $(l_\delta^{\text{KL3}}, u_\delta^{\text{KL3}})$, we have

$$\begin{aligned}
& \frac{1}{d^{\pi_{\theta_{\text{old}}}(s)}} \frac{\partial}{\partial \theta_{s,a}} \mathcal{J}^{\text{ATR}}(\theta) \\
&= \mathbb{P}(A > 0, l_\delta^{\text{KL3}} \leq w_t(\theta_{s,a'}) \leq u_\delta^{\text{KL3}}) \mathbb{E}_{a' \sim \pi_{\theta_{\text{old}}}(\cdot|s)} \left[\frac{\partial}{\partial \theta_{s,a}} w_t(\theta_{s,a'}) A | A > 0, l_\delta^{\text{KL3}} \leq w_t(\theta_{s,a'}) \leq u_\delta^{\text{KL3}} \right] \\
&+ \mathbb{P}(A > 0, w_t(\theta_{s,a'}) \leq l_\delta^{\text{KL3}}) \mathbb{E}_{a' \sim \pi_{\theta_{\text{old}}}(\cdot|s)} \left[\frac{\partial}{\partial \theta_{s,a}} l_\delta^{\text{KL3}} A | A > 0, w_t(\theta_{s,a'}) \leq l_\delta^{\text{KL3}} \right] \\
&+ \mathbb{P}(A > 0, w_t(\theta_{s,a'}) \geq u_\delta^{\text{KL3}}) \mathbb{E}_{a' \sim \pi_{\theta_{\text{old}}}(\cdot|s)} \left[\frac{\partial}{\partial \theta_{s,a}} u_\delta^{\text{KL3}} A | A > 0, w_t(\theta_{s,a'}) \geq u_\delta^{\text{KL3}} \right] \\
&+ \mathbb{P}(A < 0, l_\delta^{\text{KL3}} \leq w_t(\theta_{s,a'}) \leq u_\delta^{\text{KL3}}) \mathbb{E}_{a' \sim \pi_{\theta_{\text{old}}}(\cdot|s)} \left[\frac{\partial}{\partial \theta_{s,a}} w_t(\theta_{s,a'}) A | A < 0, l_\delta^{\text{KL3}} \leq w_t(\theta_{s,a'}) \leq u_\delta^{\text{KL3}} \right] \quad (16) \\
&+ \mathbb{P}(A < 0, w_t(\theta_{s,a'}) \leq l_\delta^{\text{KL3}}) \mathbb{E}_{a' \sim \pi_{\theta_{\text{old}}}(\cdot|s)} \left[\frac{\partial}{\partial \theta_{s,a}} l_\delta^{\text{KL3}} A | A < 0, w_t(\theta_{s,a'}) \leq l_\delta^{\text{KL3}} \right] \\
&+ \mathbb{P}(A < 0, w_t(\theta_{s,a'}) \geq u_\delta^{\text{KL3}}) \mathbb{E}_{a' \sim \pi_{\theta_{\text{old}}}(\cdot|s)} \left[\frac{\partial}{\partial \theta_{s,a}} u_\delta^{\text{KL3}} A | A < 0, w_t(\theta_{s,a'}) \geq u_\delta^{\text{KL3}} \right] \\
&= \mathbb{P}(A > 0, l_\delta^{\text{KL3}} \leq w_t(\theta_{s,a'}) \leq u_\delta^{\text{KL3}}) \mathbb{E}_{a' \sim \pi_{\theta_{\text{old}}}(\cdot|s)} \left[\frac{\partial}{\partial \theta_{s,a}} w_t(\theta_{s,a'}) A | A > 0, l_\delta^{\text{KL3}} \leq w_t(\theta_{s,a'}) \leq u_\delta^{\text{KL3}} \right] \\
&+ \mathbb{P}(A < 0, l_\delta^{\text{KL3}} \leq w_t(\theta_{s,a'}) \leq u_\delta^{\text{KL3}}) \mathbb{E}_{a' \sim \pi_{\theta_{\text{old}}}(\cdot|s)} \left[\frac{\partial}{\partial \theta_{s,a}} w_t(\theta_{s,a'}) A | A < 0, l_\delta^{\text{KL3}} \leq w_t(\theta_{s,a'}) \leq u_\delta^{\text{KL3}} \right].
\end{aligned}$$

Similarly, for the ratio-based clipping $(1 - \epsilon, 1 + \epsilon)$, we have

$$\begin{aligned}
& \frac{1}{d^{\pi_{\theta_{\text{old}}}(s)}} \frac{\partial}{\partial \theta_{s,a}} \mathcal{J}^{\text{ratio}}(\theta) \\
&= \mathbb{P}(A > 0, 1 - \epsilon \leq w_t(\theta_{s,a'}) \leq 1 + \epsilon) \mathbb{E}_{a' \sim \pi_{\theta_{\text{old}}}(\cdot|s)} \left[\frac{\partial}{\partial \theta_{s,a}} w_t(\theta_{s,a'}) A | A > 0, 1 - \epsilon \leq w_t(\theta_{s,a'}) \leq 1 + \epsilon \right] \quad (17) \\
&+ \mathbb{P}(A < 0, 1 - \epsilon \leq w_t(\theta_{s,a'}) \leq 1 + \epsilon) \mathbb{E}_{a' \sim \pi_{\theta_{\text{old}}}(\cdot|s)} \left[\frac{\partial}{\partial \theta_{s,a}} w_t(\theta_{s,a'}) A | A < 0, 1 - \epsilon \leq w_t(\theta_{s,a'}) \leq 1 + \epsilon \right].
\end{aligned}$$

Since we apply the policy gradient algorithm, and we have that

$$\begin{aligned}
\theta_{s,a}^{\text{ATR},k+1} - \theta_{s,a}^k &= \eta \frac{\partial}{\partial \theta_{s,a}} \mathcal{J}^{\text{ATR}}(\theta) \\
\theta_{s,a}^{\text{ratio},k+1} - \theta_{s,a}^k &= \eta \frac{\partial}{\partial \theta_{s,a}} \mathcal{J}^{\text{ratio}}(\theta)
\end{aligned} \quad (18)$$

Then, we have

$$\begin{aligned}
& \frac{1}{\eta d^{\pi_{\theta_{\text{old}}}(s)}} (\theta_{s,a}^{\text{ATR},k+1} - \theta_{s,a}^{\text{ratio},k+1}) \\
&= \mathbb{P}(A > 0, l_\delta^{\text{KL3}} \leq w_t(\theta_{s,a'}) \leq u_\delta^{\text{KL3}}) \mathbb{E}_{a' \sim \pi_{\theta_{\text{old}}}(\cdot|s)} \left[\frac{\partial}{\partial \theta_{s,a}} w_t(\theta_{s,a'}) A | A > 0, l_\delta^{\text{KL3}} \leq w_t(\theta_{s,a'}) \leq u_\delta^{\text{KL3}} \right] \\
&- \mathbb{P}(A > 0, 1 - \epsilon \leq w_t(\theta_{s,a'}) \leq 1 + \epsilon) \mathbb{E}_{a' \sim \pi_{\theta_{\text{old}}}(\cdot|s)} \left[\frac{\partial}{\partial \theta_{s,a}} w_t(\theta_{s,a'}) A | A > 0, 1 - \epsilon \leq w_t(\theta_{s,a'}) \leq 1 + \epsilon \right] \quad (19) \\
&+ \mathbb{P}(A < 0, l_\delta^{\text{KL3}} \leq w_t(\theta_{s,a'}) \leq u_\delta^{\text{KL3}}) \mathbb{E}_{a' \sim \pi_{\theta_{\text{old}}}(\cdot|s)} \left[\frac{\partial}{\partial \theta_{s,a}} w_t(\theta_{s,a'}) A | A < 0, l_\delta^{\text{KL3}} \leq w_t(\theta_{s,a'}) \leq u_\delta^{\text{KL3}} \right] \\
&- \mathbb{P}(A < 0, 1 - \epsilon \leq w_t(\theta_{s,a'}) \leq 1 + \epsilon) \mathbb{E}_{a' \sim \pi_{\theta_{\text{old}}}(\cdot|s)} \left[\frac{\partial}{\partial \theta_{s,a}} w_t(\theta_{s,a'}) A | A < 0, 1 - \epsilon \leq w_t(\theta_{s,a'}) \leq 1 + \epsilon \right]
\end{aligned}$$

Now, we consider the first case: $u_\delta^{\text{KL3}} = 1 + \epsilon$ and $1 - \epsilon < l_\delta^{\text{KL3}}$. In this case, we have

$$\begin{aligned}
& \mathbb{P}(A > 0, l_\delta^{\text{KL3}} \leq w_t(\theta_{s,a'}) \leq u_\delta^{\text{KL3}}) \mathbb{E}_{a' \sim \pi_{\theta_{\text{old}}}(\cdot|s)} \left[\frac{\partial}{\partial \theta_{s,a}} w_t(\theta_{s,a'}) A | A > 0, l_\delta^{\text{KL3}} \leq w_t(\theta_{s,a'}) \leq u_\delta^{\text{KL3}} \right] \\
& - \mathbb{P}(A > 0, 1 - \epsilon \leq w_t(\theta_{s,a'}) \leq u_\delta^{\text{KL3}}) \mathbb{E}_{a' \sim \pi_{\theta_{\text{old}}}(\cdot|s)} \left[\frac{\partial}{\partial \theta_{s,a}} w_t(\theta_{s,a'}) A | A > 0, 1 - \epsilon \leq w_t(\theta_{s,a'}) \leq u_\delta^{\text{KL3}} \right] \\
& = \mathbb{P}(A > 0, l_\delta^{\text{KL3}} \leq w_t(\theta_{s,a'}) \leq u_\delta^{\text{KL3}}) \mathbb{E}_{a' \sim \pi_{\theta_{\text{old}}}(\cdot|s)} \left[\frac{\partial}{\partial \theta_{s,a}} w_t(\theta_{s,a'}) A | A > 0, l_\delta^{\text{KL3}} \leq w_t(\theta_{s,a'}) \leq u_\delta^{\text{KL3}} \right] \\
& - \mathbb{P}(A > 0, 1 - \epsilon \leq w_t(\theta_{s,a'}) \leq l_\delta^{\text{KL3}}) \mathbb{E}_{a' \sim \pi_{\theta_{\text{old}}}(\cdot|s)} \left[\frac{\partial}{\partial \theta_{s,a}} w_t(\theta_{s,a'}) A | A > 0, 1 - \epsilon \leq w_t(\theta_{s,a'}) \leq l_\delta^{\text{KL3}} \right] \\
& - \mathbb{P}(A > 0, l_\delta^{\text{KL3}} \leq w_t(\theta_{s,a'}) \leq u_\delta^{\text{KL3}}) \mathbb{E}_{a' \sim \pi_{\theta_{\text{old}}}(\cdot|s)} \left[\frac{\partial}{\partial \theta_{s,a}} w_t(\theta_{s,a'}) A | A > 0, l_\delta^{\text{KL3}} \leq w_t(\theta_{s,a'}) \leq u_\delta^{\text{KL3}} \right] \\
& = - \mathbb{P}(A > 0, 1 - \epsilon \leq w_t(\theta_{s,a'}) \leq l_\delta^{\text{KL3}}) \mathbb{E}_{a' \sim \pi_{\theta_{\text{old}}}(\cdot|s)} \left[\frac{\partial}{\partial \theta_{s,a}} w_t(\theta_{s,a'}) A | A > 0, 1 - \epsilon \leq w_t(\theta_{s,a'}) \leq l_\delta^{\text{KL3}} \right]
\end{aligned} \tag{20}$$

Similarly, we have

$$\begin{aligned}
& \mathbb{P}(A < 0, l_\delta^{\text{KL3}} \leq w_t(\theta_{s,a'}) \leq u_\delta^{\text{KL3}}) \mathbb{E}_{a' \sim \pi_{\theta_{\text{old}}}(\cdot|s)} \left[\frac{\partial}{\partial \theta_{s,a}} w_t(\theta_{s,a'}) A | A < 0, l_\delta^{\text{KL3}} \leq w_t(\theta_{s,a'}) \leq u_\delta^{\text{KL3}} \right] \\
& - \mathbb{P}(A < 0, 1 - \epsilon \leq w_t(\theta_{s,a'}) \leq u_\delta^{\text{KL3}}) \mathbb{E}_{a' \sim \pi_{\theta_{\text{old}}}(\cdot|s)} \left[\frac{\partial}{\partial \theta_{s,a}} w_t(\theta_{s,a'}) A | A < 0, 1 - \epsilon \leq w_t(\theta_{s,a'}) \leq u_\delta^{\text{KL3}} \right] \\
& = - \mathbb{P}(A < 0, 1 - \epsilon \leq w_t(\theta_{s,a'}) \leq l_\delta^{\text{KL3}}) \mathbb{E}_{a' \sim \pi_{\theta_{\text{old}}}(\cdot|s)} \left[\frac{\partial}{\partial \theta_{s,a}} w_t(\theta_{s,a'}) A | A < 0, 1 - \epsilon \leq w_t(\theta_{s,a'}) \leq l_\delta^{\text{KL3}} \right]
\end{aligned} \tag{21}$$

Therefore, we have

$$\begin{aligned}
& \frac{1}{\eta d^{\pi_{\theta_{\text{old}}}(s)}} (\theta_{s,a}^{\text{ATR},k+1} - \theta_{s,a}^{\text{ratio},k+1}) \\
& = - \mathbb{P}(A > 0, 1 - \epsilon \leq w_t(\theta_{s,a'}) \leq l_\delta^{\text{KL3}}) \mathbb{E}_{a' \sim \pi_{\theta_{\text{old}}}(\cdot|s)} \left[\frac{\partial}{\partial \theta_{s,a}} w_t(\theta_{s,a'}) A | A > 0, 1 - \epsilon \leq w_t(\theta_{s,a'}) \leq l_\delta^{\text{KL3}} \right] \\
& - \mathbb{P}(A < 0, 1 - \epsilon \leq w_t(\theta_{s,a'}) \leq l_\delta^{\text{KL3}}) \mathbb{E}_{a' \sim \pi_{\theta_{\text{old}}}(\cdot|s)} \left[\frac{\partial}{\partial \theta_{s,a}} w_t(\theta_{s,a'}) A | A < 0, 1 - \epsilon \leq w_t(\theta_{s,a'}) \leq l_\delta^{\text{KL3}} \right] \\
& = - \mathbb{P}(1 - \epsilon \leq w_t(\theta_{s,a'}) \leq l_\delta^{\text{KL3}}) \mathbb{E}_{a' \sim \pi_{\theta_{\text{old}}}(\cdot|s)} \left[\frac{\partial}{\partial \theta_{s,a}} w_t(\theta_{s,a'}) A | 1 - \epsilon \leq w_t(\theta_{s,a'}) \leq l_\delta^{\text{KL3}} \right]
\end{aligned} \tag{22}$$

Due to we have

$$\frac{\partial}{\partial \theta_{s,a}} w_t(\theta_{s,a'}) = \mathbb{I}_{\{a=a'\}} \frac{\pi_{\theta^k}(a|s)}{\pi_{\theta_{\text{old}}}(a'|s)} - \pi_{\theta^k}(a|s) \frac{\pi_{\theta^k}(a'|s)}{\pi_{\theta_{\text{old}}}(a'|s)} \tag{23}$$

We assume the event

$$X_-(s) = \{a \in \mathcal{A}(s) | w_t(\theta_{s,a}) \in [1 - \epsilon, l_\delta^{\text{KL3}}], 1 + \epsilon = u_\delta^{\text{KL3}}\} \tag{24}$$

Then

$$\begin{aligned}
& \theta_{s,a}^{\text{ATR},k+1} - \theta_{s,a}^{\text{ratio},k+1} \\
&= -\eta d^{\pi_{\theta_{\text{old}}}(s)} \mathbb{P}(1 - \epsilon \leq w_t(\theta_{s,a'}) \leq l_{\delta}^{\text{KL3}}) \mathbb{E}_{a' \sim \pi_{\theta_{\text{old}}}(\cdot|s)} \left[\frac{\partial}{\partial \theta_{s,a}} w_t(\theta_{s,a'}) A | 1 - \epsilon \leq w_t(\theta_{s,a'}) \leq l_{\delta}^{\text{KL3}} \right] \\
&= -\eta d^{\pi_{\theta_{\text{old}}}(s)} \mathbb{E}_{a' \sim \pi_{\theta_{\text{old}}}(\cdot|s)} \left[\frac{\partial}{\partial \theta_{s,a}} w_t(\theta_{s,a'}) A \mathbb{I}_{X_-(s)}(a') \right] \\
&= -\eta d^{\pi_{\theta_{\text{old}}}(s)} \sum_{a' \in \mathcal{A}(s)} \left[(\mathbb{I}_{\{a=a'\}} \pi_{\theta^k}(a|s) - \pi_{\theta^k}(a|s) \pi_{\theta^k}(a'|s)) A \mathbb{I}_{X_-(s)}(a') \right] \\
&= -\eta d^{\pi_{\theta_{\text{old}}}(s)} \left[\pi_{\theta^k}(a|s) A \mathbb{I}_{X_-(s)}(a) - \pi_{\theta^k}(a|s) \mathbb{E}_{a' \sim \pi_{\theta^k}(\cdot|s)} [A \mathbb{I}_{X_-(s)}(a')] \right] \\
&= -\eta d^{\pi_{\theta_{\text{old}}}(s)} \pi_{\theta^k}(a|s) \left[A \mathbb{I}_{X_-(s)}(a) - \mathbb{E}_{a' \sim \pi_{\theta^k}(\cdot|s)} [A \mathbb{I}_{X_-(s)}(a')] \right]
\end{aligned} \tag{25}$$

Then, we consider the second case: $l_{\delta}^{\text{KL3}} = 1 - \epsilon$ and $1 + \epsilon < u_{\delta}^{\text{KL3}}$. We assume the event

$$X_+(s) = \{a \in \mathcal{A}(s) | w_t(\theta_{s,a}) \in [1 + \epsilon, u_{\delta}^{\text{KL3}}], 1 - \epsilon = l_{\delta}^{\text{KL3}}\} \tag{26}$$

Similarly, in this case, we have

$$\begin{aligned}
& \theta_{s,a}^{\text{ATR},k+1} - \theta_{s,a}^{\text{ratio},k+1} \\
&= \eta d^{\pi_{\theta_{\text{old}}}(s)} \mathbb{P}(1 + \epsilon \leq w_t(\theta_{s,a'}) \leq u_{\delta}^{\text{KL3}}) \mathbb{E}_{a' \sim \pi_{\theta_{\text{old}}}(\cdot|s)} \left[\frac{\partial}{\partial \theta_{s,a}} w_t(\theta_{s,a'}) A | 1 + \epsilon \leq w_t(\theta_{s,a'}) \leq u_{\delta}^{\text{KL3}} \right] \\
&= \eta d^{\pi_{\theta_{\text{old}}}(s)} \pi_{\theta^k}(a|s) \left[A \mathbb{I}_{X_+(s)}(a) - \mathbb{E}_{a' \sim \pi_{\theta^k}(\cdot|s)} [A \mathbb{I}_{X_+(s)}(a')] \right]
\end{aligned} \tag{27}$$

□

A.3. Entropy Difference Analysis

Theorem A.3 (Entropy Difference). Let $\Delta \mathcal{H} := \mathcal{H}(\theta^{\text{ATR},k+1}|s) - \mathcal{H}(\theta^{\text{ratio},k+1}|s)$ denote the entropy difference between the ATR-based and ratio-based clipping methods.

Under event $X_-(s)$, we have $\Delta \mathcal{H} = \eta d^{\pi_{\theta_{\text{old}}}(s)} \text{Cov}_{a \sim \pi_{\theta^k}(\cdot|s)} (A \mathbb{I}_{X_-(s)}(a), \log \pi_{\theta^k}(a|s))$.

Under event $X_+(s)$, we have $\Delta \mathcal{H} = -\eta d^{\pi_{\theta_{\text{old}}}(s)} \text{Cov}_{a \sim \pi_{\theta^k}(\cdot|s)} (A \mathbb{I}_{X_+(s)}(a), \log \pi_{\theta^k}(a|s))$.

Proof. The first-order Taylor expansion of policy entropy

$$\mathcal{H}(\theta^{k+1}|s) - \mathcal{H}(\theta^k|s) = -\mathbb{E}_{a \sim \pi_{\theta^k}(\cdot|s)} [(\theta_{s,a}^{k+1} - \theta_{s,a}^k) (\log \pi_{\theta^k}(a|s) + \mathcal{H}(\theta^k|s))] + \mathcal{O}((\Delta \theta)^2) \tag{28}$$

Consider that we have two different clipping methods with corresponding $\theta^{\text{ratio},k+1}$ and $\theta^{\text{ATR},k+1}$

$$\begin{aligned}
& \mathcal{H}(\theta^{\text{ATR},k+1}|s) - \mathcal{H}(\theta^{\text{ratio},k+1}|s) \\
&= (\mathcal{H}(\theta^{\text{ATR},k+1}|s) - \mathcal{H}(\theta^k|s)) - (\mathcal{H}(\theta^{\text{ratio},k+1}|s) - \mathcal{H}(\theta^k|s)) \\
&= -\mathbb{E}_{a \sim \pi_{\theta^k}(\cdot|s)}[(\theta_{s,a}^{\text{ATR},k+1} - \theta_{s,a}^k)(\log \pi_{\theta^k}(a|s) + \mathcal{H}(\theta^k|s))] + \mathbb{E}_{a \sim \pi_{\theta^k}(\cdot|s)}[(\theta_{s,a}^{\text{ratio},k+1} - \theta_{s,a}^k)(\log \pi_{\theta^k}(a|s) + \mathcal{H}(\theta^k|s))] \\
&= -\mathbb{E}_{a \sim \pi_{\theta^k}(\cdot|s)}[(\theta_{s,a}^{\text{ATR},k+1} - \theta_{s,a}^{\text{ratio},k+1})(\log \pi_{\theta^k}(a|s) + \mathcal{H}(\theta^k|s))] \\
&= -\mathbb{E}_{a \sim \pi_{\theta^k}(\cdot|s)}[(\theta_{s,a}^{\text{ATR},k+1} - \theta_{s,a}^{\text{ratio},k+1})(\log \pi_{\theta^k}(a|s) - \mathbb{E}_{a' \sim \pi_{\theta^k}(\cdot|s)}[\log \pi_{\theta^k}(a'|s)])]
\end{aligned} \tag{29}$$

For the event $X_-(s)$, we have

$$\begin{aligned}
& \mathcal{H}(\theta^{\text{ATR},k+1}|s) - \mathcal{H}(\theta^{\text{ratio},k+1}|s) \\
&= -\mathbb{E}_{a \sim \pi_{\theta^k}(\cdot|s)} \left[\left(-\eta d^{\pi_{\theta^{\text{old}}}(s)} \pi_{\theta^k}(a|s) \left[A \mathbb{I}_{X_-(s)}(a) - \mathbb{E}_{a' \sim \pi_{\theta^k}(\cdot|s)}[A \mathbb{I}_{X_-(s)}(a')] \right] \right) \left(\log \pi_{\theta^k}(a|s) - \mathbb{E}_{a' \sim \pi_{\theta^k}(\cdot|s)}[\log \pi_{\theta^k}(a'|s)] \right) \right] \\
&= \eta d^{\pi_{\theta^{\text{old}}}(s)} \mathbb{E}_{a \sim \pi_{\theta^k}(\cdot|s)} \left(A \mathbb{I}_{X_-(s)}(a), \log \pi_{\theta^k}(a|s) \right) \\
&\quad \mathbb{E}_{a \sim \pi_{\theta^k}(\cdot|s)} \left(\log \pi_{\theta^k}(a|s) - \mathbb{E}_{a' \sim \pi_{\theta^k}(\cdot|s)}[\log \pi_{\theta^k}(a'|s)] \right)
\end{aligned} \tag{30}$$

For the event $X_+(s)$, we have

$$\begin{aligned}
& \mathcal{H}(\theta^{\text{ATR},k+1}|s) - \mathcal{H}(\theta^{\text{ratio},k+1}|s) \\
&= -\mathbb{E}_{a \sim \pi_{\theta^k}(\cdot|s)} \left[\left(\eta d^{\pi_{\theta^{\text{old}}}(s)} \pi_{\theta^k}(a|s) \left[A \mathbb{I}_{X_+(s)}(a) - \mathbb{E}_{a' \sim \pi_{\theta^k}(\cdot|s)}[A \mathbb{I}_{X_+(s)}(a')] \right] \right) \left(\log \pi_{\theta^k}(a|s) - \mathbb{E}_{a' \sim \pi_{\theta^k}(\cdot|s)}[\log \pi_{\theta^k}(a'|s)] \right) \right] \\
&= -\eta d^{\pi_{\theta^{\text{old}}}(s)} \mathbb{E}_{a \sim \pi_{\theta^k}(\cdot|s)} \left(A \mathbb{I}_{X_+(s)}(a), \log \pi_{\theta^k}(a|s) \right) \\
&\quad \mathbb{E}_{a \sim \pi_{\theta^k}(\cdot|s)} \left(\log \pi_{\theta^k}(a|s) - \mathbb{E}_{a' \sim \pi_{\theta^k}(\cdot|s)}[\log \pi_{\theta^k}(a'|s)] \right)
\end{aligned} \tag{31}$$

□

B. Implementation Details

The hyper-parameter setting used in this work is provided in Table 4. Following recent works (Hu et al., 2025; Liu et al., 2025c), we set $\beta = 0$ for all methods. We adopt the official implementation from Unslot (Daniel Han & team, 2023) and TRL (von Werra et al., 2020). For all methods, we perform the supervised fine-tuning on the OpenMathReasoning dataset (Moshkov et al., 2025) for formatting before the RLVR process. We provide the full codebase used to reproduce our experimental results in the supplementary material. On one single NVIDIA A100 GPU, ATR-GRPO requires an average training time of approximately 7 and 16 hours per run for Qwen3-1.7B and Qwen3-8B, respectively. For the implementation of baselines, we adopt the recommended value settings from the original papers, including DAPO (Yu et al., 2025), DCPO (Yang et al., 2025b), Clip-Cov (Cui et al., 2025), and SAPO (Gao et al., 2025).

Table 4. Hyper-parameter Setting.

Hyper-Parameter	Value
	Train
Maximum Sequence Length	2048
Lora Rank	32
Lora Alpha	64
Temperature	1.0
Learning Rate	5e-6
Weight Decay	1e-3
Optimizer	AdamW (Loshchilov & Hutter, 2017)
Batch Size	8
Gradient Accumulation Steps	4
Top-p	1.0
Top-k	-1
Group Size G	8
KL coefficient β (reference policy)	0
	Evaluation
Temperature	0.3
Max Tokens	32768
Top-p	0.95
Top-k	-1